Available online at www.sciencedirect.com

ScienceDirect

Ceramics International 38 (2012) 761–767

CERAMICS INTERNATIONAL

www.elsevier.com/locate/ceramint

Microstructural characterization on ZrC doped carbon/carbon composites

Zhou Chen, Wangping Wu, Zhaofeng Chen *, Xiangna Cong, Jinlian Qiu

College of Material Science and Technology, Nanjing University of Aeronautics and Astronautics, Nanjing 210016, PR China

Received 25 April 2011; received in revised form 30 July 2011; accepted 1 August 2011

Available online 9th August 2011

Abstract

Zirconium carbide doped carbon/carbon (ZrC–C/C) composites were prepared by the polymer impregnation and pyrolysis process. Carbon fiber preforms were firstly immersed into zirconium acetate solution/phenolic resin impregnant, and then carbonized at 1000 °C. After four cycles of impregnation/carbonization, they were finally graphitized at 2000 °C. The phase composition of the composites was examined by X-ray diffraction. Microstructural characterization of the composites were investigated by scanning electron microscopy and transmission electron microscopy. The results indicated that ZrC particles with sub-micron size were well dispersed in carbon matrix. ZrC particles were encapsulated by highly oriented carbon, and there existed a well bonded interface between ZrC particles and highly oriented carbon. The formation mechanism of the encapsulated structure was proposed.

Keywords: A: Precursor: organic; B: Composites; Microstructure; ZrC

1. Introduction

Carbon/carbon (C/C) composites have many unique properties, such as low density, low coefficient of thermal expansion, high thermal conductivity, high modulus and good thermal shock resistance [1–3]. These outstanding properties make C/C composites one of the most promising candidates for high temperature applications such as rocket nozzles, re-entry heat shields, nose tips and leading edges [4]. However, the use of C/C composites has been limited because of oxidation above 500 °C in air [5]. It is necessary to improve oxidation resistance for C/C composites in oxidizing atmosphere at high temperature.

It has been proved effectively to improve the oxidation resistance of C/C composites by doping refractory carbides such as zirconium carbide (ZrC), hafnium carbide (HfC) and tantalum carbide (TaC) [6]. ZrC is an advanced ceramic with a high melting point (3540 °C), great hardness (25.5 GPa) and excellent mechanical stability [7,8]. Compared to HfC (12.7 g/cm^3) or TaC (14.5 g/cm^3), ZrC has a lower density (6.59 g/cm^3) [7,8]. Adding a certain amount of ZrC in C/C composites can get higher degree of graphitization and thermal conductivity, better mechanical properties and oxidation resistance at a certain heat treatment temperature [9–11]. The formation of the zirconia (ZrO_2) layer, which is caused by the oxidation of the doped ZrC, is good to improve the anti-ablation property of C/C composites. It effectively reduce the diffusion of oxygen and the ablation rate. ZrC doped C/C (ZrC–C/C) composites can be used as a new high-temperature structural materials.

Scientists have been looking for many methods to obtain ZrC–C/C composites. Tong et al. [12] prepared pitch-derived ZrC/C composites using Zr-containing pitch and petroleum by hot-pressed technology. Gao et al. [11] prepared C/C composites containing ZrC using chopped carbon fiber, mesophase pitch and Zr powder by the traditional process including molding, carbonization, densification and graphitization. Shen et al. [13] reported that ZrC doped C/C composites were produced by a series of procedures combined with carbon felt immersing in zirconium oxychloride aqueous solution, densification by thermal gradient chemical vapor infiltration and then graphitization.

In this paper, ZrC–C/C composites were prepared by the polymer impregnation and pyrolysis process. The microstructural characterization on the ZrC–C/C composites was deeply investigated.

---

* Corresponding author. Tel.: +86 25 52112909; fax: +86 25 52112626.
E-mail address: zhaofeng_chen@163.com (Z. Chen).

0272-8842/$36.00. Crown Copyright © 2011 Published by Elsevier Ltd and Techna Group S.r.l. All rights reserved.
doi:10.1016/j.ceramint.2011.08.002

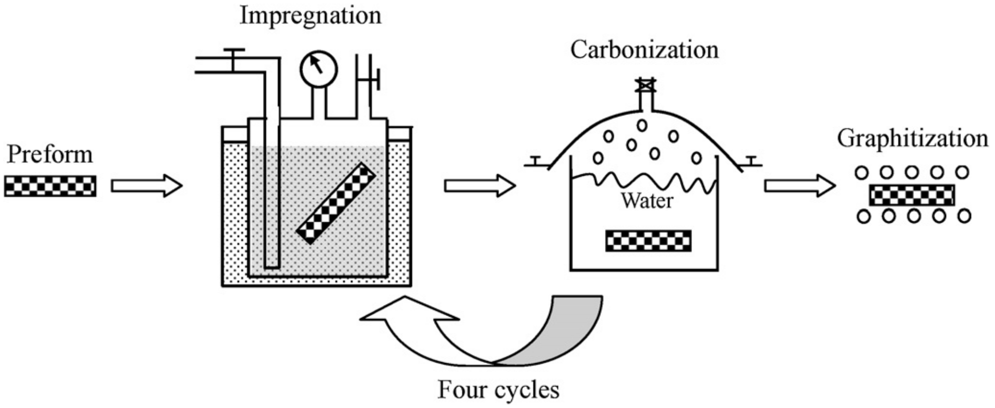

Fig. 1. Schematic preparation procedures of ZrC–C/C composites.

2. Experimental

2.1. Sample preparation

The needled carbon fiber preform fabricated by T300 PAN-based carbon fibers (Toray, Japan) was formed by alternatively stacked weftless plies and short-cut-fiber webs with a needle-punching technique in *Z* direction. The impregnant was prepared by mixing a certain amount of zirconium acetate solution and phenolic resin, and heating to 100 °C under the protection of nitrogen atmosphere.

Fig. 1 shows the schematic preparation procedure of ZrC–C/C composites. The preform was impregnated in the impregnant for 2 h and dried. The dried preform was placed in a furnace and carbonized at 1000 °C in nitrogen atmosphere for 0.5 h. After four general impregnation/carbonization cycles, the samples were finally obtained by graphitization at 2000 °C in argon atmosphere for 0.5 h.

2.2. Characterization

The phase identification of the composites was examined by X-ray diffraction (XRD, Rigaku D/Max-B) using Ni-filtered Cu Kα radiation at a scanning rate of 4°/min and scanning from 10° to 100° of 2θ. Microstructural characterization of the composites were observed by scanning electron microscopy (SEM, JEOL, JSM-6360) and transmission electron microscopy (TEM, 200KV Tecnai G2 20). TEM samples were prepared by grinding a bulk sample of ZrC–C/C composites to about 50 μm in thickness and then a 3 mm diameter disc was cut out. The disc was subsequently dimpled and ion milled. The chemical composition of the composites was analyzed by energy dispersive spectroscopy (EDS, LINK-860).

3. Results and discussion

Fig. 2 shows the XRD patterns of ZrC–C/C composites. Fig. 2(a) displays the XRD pattern of the composites carbonized at 1000 °C for 0.5 h. It was found that the composites were composed of carbon and ZrO_2. It indicated that the Zr compounds were fully converted into ZrO_2 after carbonization. The XRD pattern of the composites graphitized at 2000 °C for 0.5 h is shown in Fig. 2(b). Compared with Fig. 2(a), a sharper and higher carbon (0 0 2) peak at a slightly higher angle and some characteristic (1 0 1) and (0 0 4) peaks of graphite appeared on the XRD pattern in Fig. 2(b), which was attributed to the graphitization of phenolic resin at high temperature. On the other hand, only characteristic peaks of ZrC and carbon were observed after graphitization at 2000 °C. It indicated that ZrO_2 was fully converted into ZrC and the composites only consisted of carbon and ZrC. ZrO_2 was reported to react with graphite at a minimum temperature of 1300 and 1600 °C, and the reaction was as follows [14]:

$$ZrO_2(s) + 3C(s) = ZrC(s) + 2CO(g) \tag{1}$$

XRD crystalline parameters of the composites were calculated by the following formulas [15,16]:

$$g = (3.440 - d_{002})/(3.440 - 3.354) \tag{2}$$

$$L_a = 9.5/(d_{002} - 3.354) \tag{3}$$

where $d_{0\,0\,2}$ is the measured graphite interlayer spacing, 3.440 is the value for a carbon with no graphitic order, 3.354 is the interlayer spacing of pure graphite, g is the degree of graphitization and L_a is the average crystallite diameter. Crystalline parameters of ZrC–C/C composites were listed in Table 1. The

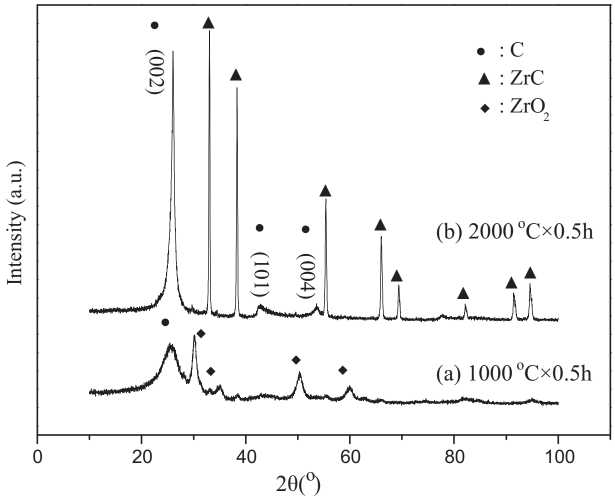

Fig. 2. XRD patterns of ZrC–C/C composites.

Table 1
Crystal parameters of ZrC–C/C composites.

Heat treatment temperature (°C)	$d_{0\,0\,2}$ (Å)	g (%)	L_a (Å)
1000	3.4267	15.46	130.7
2000	3.4122	32.3	163.2

composites graphitized at 2000 °C exhibited higher degree of graphitization and larger average crystallite diameter than those carbonized at 1000 °C. It indicated that the microstructure of the composites converted to more perfect graphite structure during the heat treatment.

Fig. 3 shows the SEM fracture micrographs and EDS patterns of ZrC–C/C composites. Fig. 3(a) displays the SEM fracture micrograph of the carbon matrix. It was found that well dispersed ZrC particles appeared in the carbon matrix of the composites. Many white ZrC particles with sub-micron size were obeserved. In fact, ZrC was not white. The white ZrC particles under SEM resulted from large contrast difference between carbon and ZrC. As shown in Fig. 3(b), the pores within the carbon filaments were filled with carbon matrix. The elemental C and Zr were detected by EDS patterns (see Fig. 3(c) and (d)), it indicated that the composites were composed of ZrC and C. The result was in agreement with that of XRD pattern (see Fig. 2(b)).

Fig. 4 shows TEM micrograph and selected area diffraction (SAED) pattern of carbon fiber. It could be seen that the carbon matrix was well-bonded to the carbon fiber, and the interface of the carbon fiber and the matrix exhibited no evidence of the delamination (see Fig. 4(a)). Some white ZrC particles presented in the carbon matrix. As illustrated in Fig. 4(b), (0 0 2), (1 0 0) and (1 1 0) planes with arc-shaped diffraction

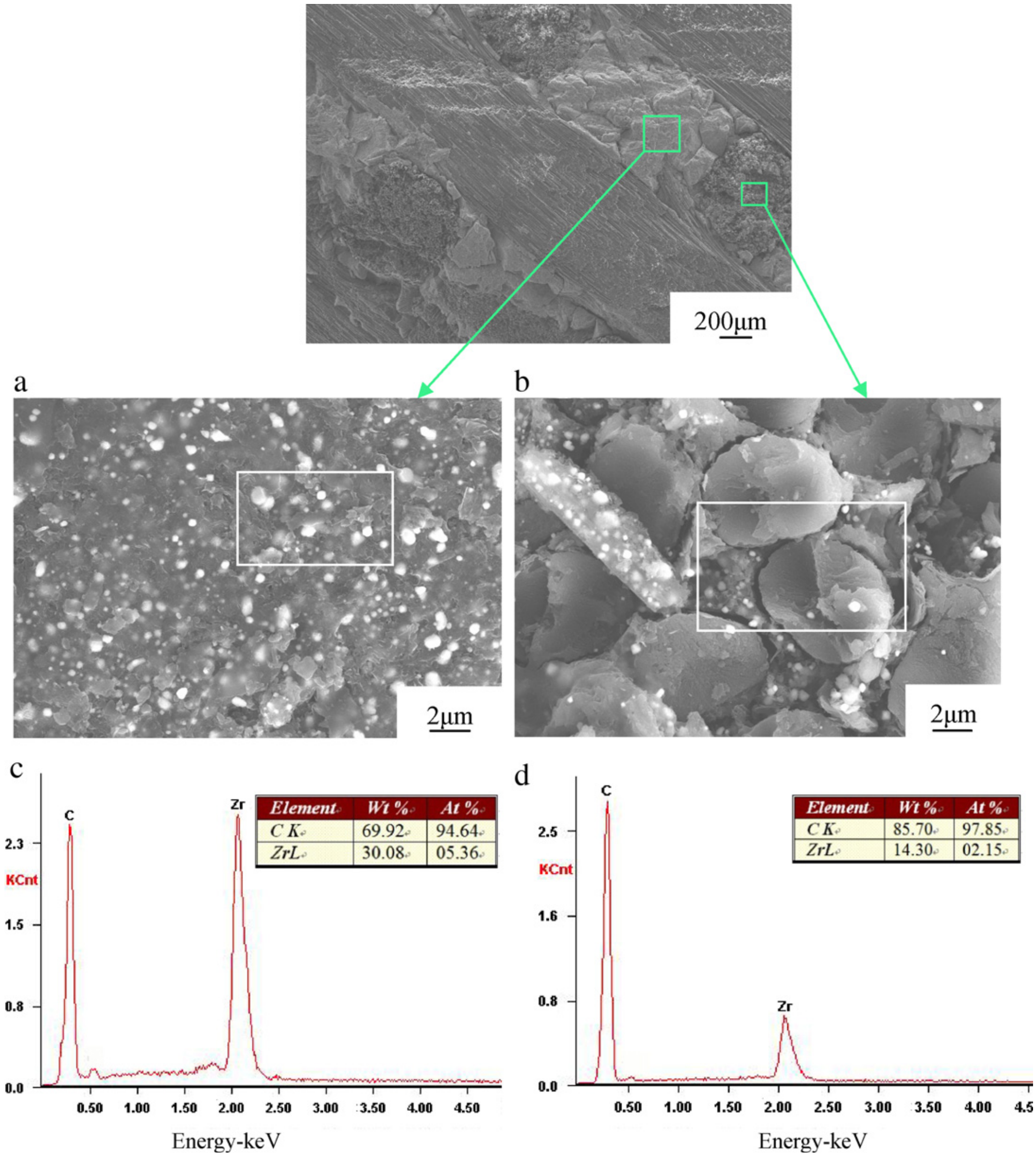

Fig. 3. SEM fracture micrographs and EDS patterns of ZrC–C/C composites.
(a) SEM fracture micrograph of carbon matrix, (b) SEM fracture micrograph of carbon fiber filaments, (c) EDS pattern of carbon matrix, (d) EDS pattern of carbon fiber filaments.

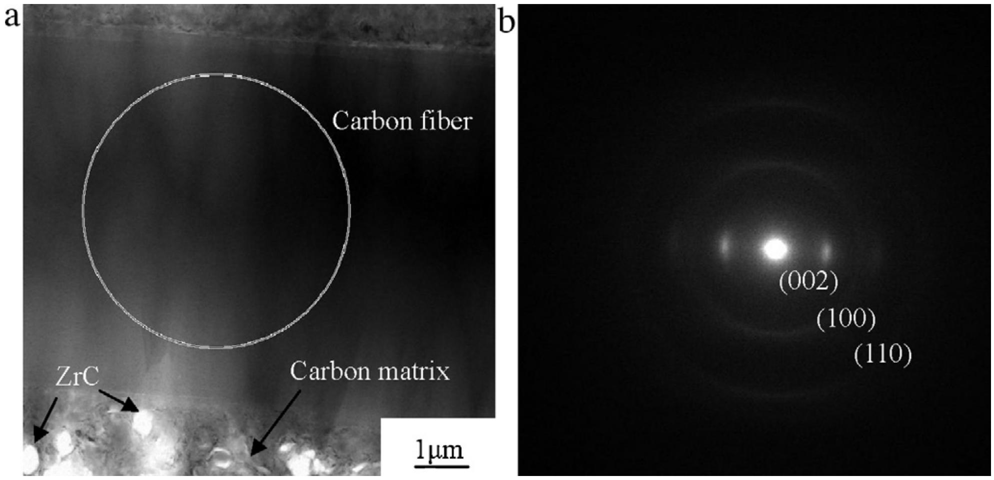

Fig. 4. TEM micrograph and SAED pattern of carbon fiber. (a) TEM micrograph of carbon fiber and (b) SAED pattern of carbon fiber.

pattern were observed, which was attributed to the carbon fiber with a high degree of graphitization [17].

Fig. 5 shows TEM micrographs and SAED patterns of the ZrC–C/C composites. As shown in Fig. 5(a), a ZrC particle with the quasi-hexagonal structure was encapsulated in carbon matrix, and a layered structure appeared around the particle. The layered structure was composed of two zones. Zone I was carbon matrix with disordered structure, Zone II was a highly

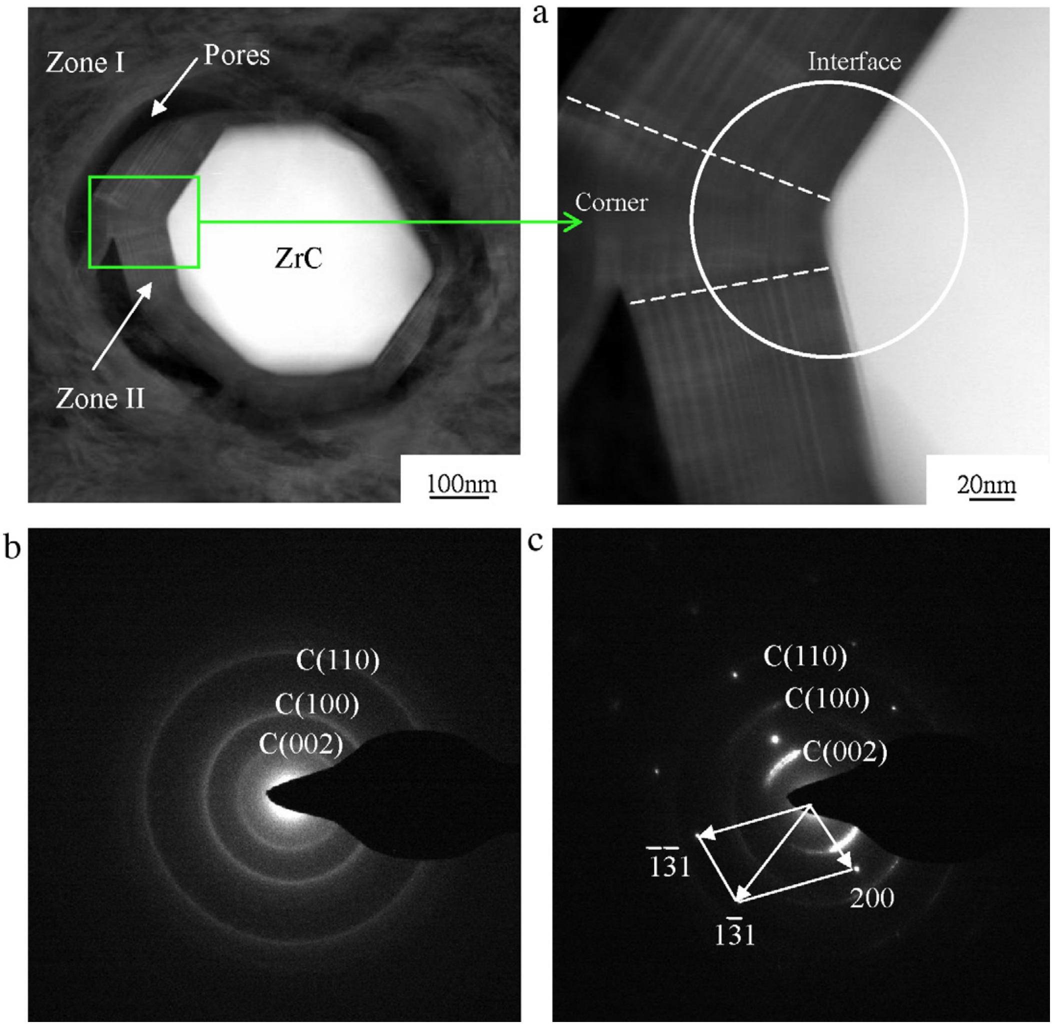

Fig. 5. TEM micrograph and SAED patterns of the ZrC–C/C composites. (a) Dark-field image, (b) SAED pattern of Zone I, (c) SAED pattern of interface area.

oriented region. The lattice fringes of Zone II orderly arrayed along the ZrC particle, and there was another lattice orientation at the corner. Some pores presented between Zones I and II might be caused by the volatilization of CO gas or the ion beam thinning during the preparation of TEM sample. Compared with the SAED of the carbon fiber (Fig. 4(b)), annular carbon diffraction pattern of the Zone I could be seen in Fig. 5(b). It was shown that carbon matrix was amorphous carbon with a low degree of graphitization [17]. Fig. 5(c) shows a spot pattern overlaid with rings of the interface area in Fig. 5(a), which indicated the crystal lattice of ZrC and the polycrystalline arc of carbon. By comparion with the SAED pattern of Fig. 5(b), the arc-shaped carbon diffraction pattern of Fig. 5(c) indicated the high degree of graphitization at the interface area [17]. It indicated that ZrC particle was encapsulated by highly oriented carbon, and there existed a well bonded interface between ZrC particle and highly oriented carbon.

Fig. 6 shows HRTEM micrographs of the interface area in Fig. 5(a). It could be observed that the interface area could be divided into two areas of A and B. For Fig. 6(b) and (c), the distance of ten selected lattice spacings of A area was 2.37 nm corresponding to (2 0 0) ZrC and the distance of ten selected lattice spacings of B area was 3.411 nm corresponding to (0 0 2) graphite.

The difference in thermal expansion coefficient between the ZrC and graphite was about 9×10^{-6} °C^{-1} [18]. Thermal stress would appear at the interface between ZrC and carbon matrix during the heat treatment temperature of 2000 °C. The stress, which was induced from thermal mismatch due to the difference of coefficient of thermal expansion between the ZrC and carbon, would induce the disordered carbon along ZrC particle to high oriented graphite. The whole catalytic graphitization process might involve a dynamic thermodynamic equilibrium between ZrC and carbon. So the formation mechanism of the encapsulated layer structure was likely to be the result of the stress graphitization. The stress-induced evolution process of the encapsulated structure is described in Fig. 7. The Zr compound was fully converted into ZrO_2 particle after carbonization. With the increasing temperature, the diffusion-reaction between ZrO_2 and amorphous carbon was accompanied by corresponding decrease of ZrO_2 particle and increase of ZrC particle (Fig. 7(b) and (c)). At the same time, CO gas volatilized and some pores were left (Fig. 7(c)). As thermal stress increased at the interface between ZrC and

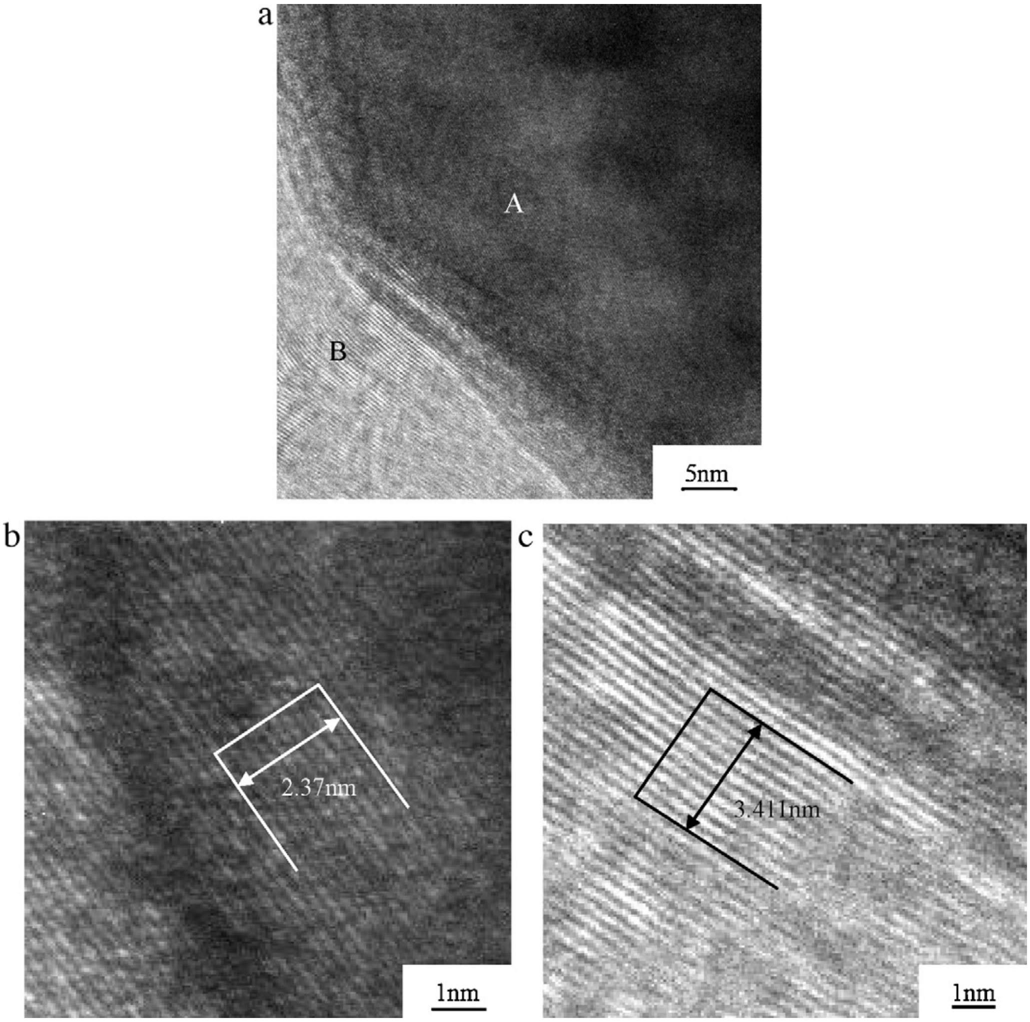

Fig. 6. HRTEM micrographs of the interface area in Fig. 5(a). (a) HRTEM micrograph of interface area, (b) HRTEM micrograph of A area, (c) HRTEM micrograph of B area.

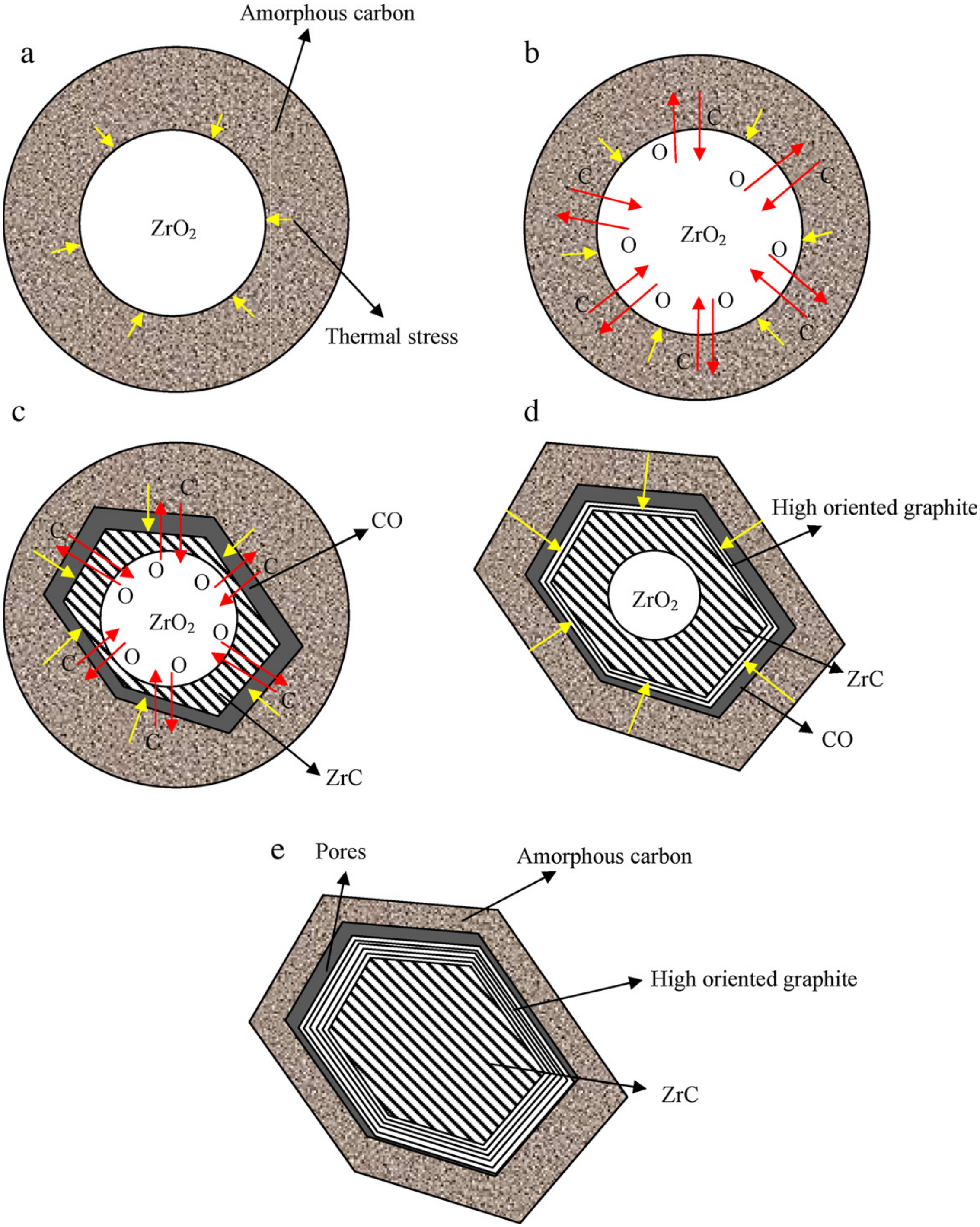

Fig. 7. Stress-induced evolution process of the encapsulated structure.

carbon matrix during the heat treatment temperature, the amorphous carbon along ZrC particle was induced to high oriented graphite (Fig. 7(d)). As shown in Fig. 7(e), the encapsulated structure composed of ZrC, high oriented graphite, pores and amorphous carbon.

4. Conclusions

ZrC–C/C composites were prepared by the polymer impregnation and pyrolysis process. The PAN-based carbon fiber preforms were firstly immersed into zirconium acetate solution/phenolic resin impregnant, and then carbonized at 1000 °C for four cycles. Finally, the densified composites were graphitized at 2000 °C for 0.5 h.

The results demonstrated the existence of two phases in the composites: carbon and ZrC. ZrC particles with sub-micron size were well dispersed in carbon matrix. ZrC particles were encapsulated by highly oriented carbon, and there existed a well bonded interface between ZrC particle and highly oriented carbon. A formation mechanism of the encapsulated layer structure was proposed. The thermal stress may induce the disordered carbon along ZrC particle to high oriented carbon.

Acknowledgements

This work has been supported by Funding for Outstanding Doctoral Dissertation in NUAA (BCXJ11-09) and Funding of Jiangsu Innovation Program for Graduate Education (CXLX11_0207).

References

[1] G. Savage, Carbon–Carbon Composites, Chapman and Hall, London; New York, 1993.

[2] E. Fitzer, L.M. Manocha, Carbon Reinforcements and Carbon/Carbon Composites, Springer, Berlin; New York, 1998, pp. 250–319.

[3] H.G. Maahs, W.L. Vaughn, W. Kowbel, Four Advances in Carbon–Carbon Materials Technology, Langley Research Center, Hampton, VA, 1994.

[4] P.O. Ransone, Y.R. Yamaki, H.G. Maahs, Recent Advances in Carbon–Carbon Substrate Technology at NASA, Langley Research Center, Hampton, VA, 1992.

[5] J.E. Sheehan, Oxidation protection for carbon fiber composites, Carbon 27 (1989) 709–715.

[6] M. Patterson, S. He, L. Fehrenbacher, B. Reed, J. Hanigofsky, Advanced HfC–TaC oxidation resistant composite rocket thruster, Mater. Manuf. Processes 11 (1996) 367–379.

[7] H.O. Pierson, Handbook of Refractory Carbides and Nitrides, Noyes Publications, Westwood, NJ, 1996.

[8] E.K. Storms, The Refractory Carbides, Academic Press, New York, 1967.

[9] H. Marsh, A.P. Warburton, Catalytic graphitization of carbon using titanium and zirconium, Carbon 14 (1976) 47–52.

[10] H.P. Qiu, L.J. Han, L. Liu, Properties and microstructure of graphitised ZrC/C or SiC/C composites, Carbon 43 (2005) 1021–1025.

[11] X.Q. Gao, L. Liu, Q.G. Guo, J.L. Shi, G.T. Zhai, The effect of zirconium addition on the microstructure and properties of chopped carbon fiber/carbon composites, Compos. Sci. Technol. 67 (2007) 525–529.

[12] Q.F. Tong, J.L. Shi, Y.Z. Song, Q.G. Guo, L. Liu, Resistance to ablation of pitch-derived ZrC/C composites, Carbon 42 (2004) 2495–2500.

[13] X.T. Shen, K.Z. Li, H.J. Li, H.Y. Du, W.F. Cao, F.T. Lan, Microstructure and ablation properties of zirconium carbide doped carbon/carbon composites, Carbon 48 (2010) 344–351.

[14] J.M. Criscione, P.A. Mercuri, A.W. Schram, A.W. Smith, H.F. Volk, High Temperature Protective Coating for Graphite, Air Force Materials Lab, Wright Patterson AFB, OH, 1964.

[15] X.Q. Gao, Q.G. Guo, J.L. Shi, G.S. Li, J.R. Song, L. Liu, The fabrication of chopped carbon fiber–carbon composites and their thermal/electrical conductivity and microstructure, New Carbon Mater. 20 (2005) 18–22.

[16] H. Takahashi, H. Kuroda, H. Akamatu, Correlation between stacking order and crystallite dimensions in carbons, Carbon 2 (1965) 432–433.

[17] V.V. Kovalevski, P.R. Buseck, J.M. Cowley, Comparison of carbon in shungite rocks to other natural carbons: an X-ray and TEM study, Carbon 39 (2001) 243–256.

[18] W.J. Gray, Design of a Capsule for Irradiating Graphite at Temperatures up to 2000 °C, Pacific Northwest Laboratory, Richland, Washington, 1980.